

1 **Immune evasion by Salmonella: Exploiting the VPAC1/VIP axis in human monocytes**

2

3 Basim Askar, John Higgins, Paul Barrow and \*Neil Foster

4

5 School of Veterinary Medicine and Science, University of Nottingham. Nottingham, UK.

6

7 \*Corresponding author:

8 Neil Foster

9 School of Veterinary Medicine and Science

10 Sutton Bonington campus

11 University of Nottingham

12 Nottingham

13 NG7 2NR

14

15 Tel: 0115 9516433

16 Email: [n.foster@nottingham.ac.uk](mailto:n.foster@nottingham.ac.uk)

17

18 **Running Title:** Salmonella exploits host VPAC1

19 **Key Words:** Salmonella VIP immune evasion Rab Calmodulin

20

21

22

23

24 **Abstract**

25 Immune evasion is a critical survival mechanism for bacterial colonization of deeper tissues and  
26 may lead to life-threatening conditions such as endotoxemia and sepsis. Understanding these  
27 immune evasion pathways would be an important step for the development of novel anti-  
28 microbial therapeutics.

29 Here, we report a hitherto unknown mechanisms by which *Salmonella* exploits an anti-  
30 inflammatory pathway in human immune cells to obtain survival advantage. We show that  
31 *Salmonella enterica* serovar Typhimurium strain 4/74 significantly ( $P < 0.05$ ) increased  
32 expression of mRNA and surface protein of the type 1 receptor (VPAC1) for anti-inflammatory  
33 vasoactive intestinal peptide (VIP) in human monocytes.

34 However, we also show that *S. Typhimurium* induced retrograde recycling of VPAC1 from early  
35 endosomes to Rab11a-containing sorting endosomes, associated with the Golgi apparatus, and  
36 anterograde trafficking via Rab3a and calmodulin 1. Expression of Rab3a and calmodulin 1 were  
37 significantly increased by *S. Typhimurium* infection and W-7 (calmodulin antagonist) decreased  
38 VPAC1 expression on the cell membrane while CALP-1 (calmodulin agonist) increased VPAC1  
39 expression ( $P < 0.05$ ). When infected monocytes were co-cultured with VIP, a significantly  
40 higher number of *S. Typhimurium* were recovered from these monocytes, compared to *S.*  
41 *Typhimurium* recovered from monocytes cultured only in cell media.

42 We conclude that *S. Typhimurium* infection exploits host VPAC1/VIP to gain survival  
43 advantage in human monocytes.

44

45

46

47 **Introduction**

48 Survival of some *Salmonella* serovars in innate immune cells is a critical step for immune  
49 evasion and colonization of deeper tissue, which may lead to life-threatening diseases such as  
50 Gram negative sepsis or typhoid. Understanding the pathways associated with immune evasion  
51 and survival may inform better therapeutic strategies for the treatment of such diseases.  
52 The bi-phasic model for human sepsis proposes a phase of uncontrolled production of  
53 inflammatory mediators, which leads to systemic inflammatory response syndrome (SIRS)  
54 followed by a compensatory anti-inflammatory response syndrome (CARS) (1-3). The SIRS  
55 (acute) phase of sepsis is associated with high systemic concentrations of pro-inflammatory  
56 cytokines released by monocytes and macrophages, such as TNF- $\alpha$ , IL-1 and IL-6 (4).  
57 Intervention with anti-inflammatories has been proposed as a rational therapeutic avenue during  
58 SIRS but specific inhibition of IL-1 $\beta$  or TNF- $\alpha$  has failed (5), while broad ranging anti-  
59 inflammatories, such as glucocorticoids, are also widely used in the treatment of sepsis but their  
60 effect is debateable, probably due to timing of therapy, dosage and the development of steroid  
61 resistance by glucocorticoid receptors (6).  
62 Studies, to date, have indicated that vasoactive intestinal peptide (VIP) may have therapeutic  
63 potential in the treatment of sepsis. The amino acid structure of VIP is highly conserved  
64 throughout the vertebrates and is identical in all mammals apart from guinea pigs (7). In murine  
65 models of LPS-induced sepsis, intra-peritoneal administration of low concentrations of VIP (<5  
66 nmol) prevented mortality and this was associated with inhibition of inflammatory cytokines (8).  
67 VIP exerts its biological effect via three G-protein coupled receptors; VIP receptor 1 (VPAC1),  
68 VPAC2 and a receptor which is also activated via the pituitary adenylate-cyclase activating  
69 polypeptide (PAC1). VPAC1 is constitutively expressed by some resting immune cells (9-10)  
70 and the immunosuppressive action of VIP on LPS-stimulated murine macrophages occurs via

71 this receptor (11). Increased VPAC1 expression was also reported in human peripheral blood  
72 monocytes following intravenous administration of LPS and correlates with increased VIP  
73 concentration in sera (12). However, using virulent *S. Typhimurium* (rather than LPS) we have  
74 shown that VIP promotes survival of *S. Typhimurium* within human monocytes, which is  
75 associated with inhibition of proinflammatory cytokines and increased survival of the infected  
76 cells (13). This may indicate that *S. Typhimurium* increases receptivity of monocytes to VIP,  
77 specifically to inhibit production of inflammatory mediators, thus gaining survival advantage. It  
78 is known that upon activation, VPAC1 is internalized and may be recycled back to the cell  
79 membrane (14-16) but nothing is known about the intracellular pathways utilized to achieve this  
80 and nothing has been reported regarding the effect of *Salmonella* infection on VPAC1 or these  
81 pathways.

82 The aim of this current study was to investigate whether *S. Typhimurium* induces VPAC1  
83 expression in human monocytes, and, if so, to determine the intracellular pathways responsible  
84 for this.

85

## 86 **Material and methods**

### 87 **Reagents**

88 Unless otherwise stated all reagents were purchased from Sigma-Aldrich, Poole, Dorset UK.

89 PCR and microarray reagents were purchased from Qiagen, Manchester, UK.

### 90 **Bioethics**

91 Human blood used in this study was obtained with patient consent. All studies were conducted  
92 following approval by local ethics committees. Studies were performed on 5 separate occasions,  
93 therefore blood from 5 individual humans.

94 **Bacterial culture and strains.**

95 *S. Typhimurium* 4/74 (17) were grown in Luria-Bertani (LB) broth (Life Technologies Ltd.,  
96 Paisley, United Kingdom) for 18 h at 37°C under agitation. The bacteria were then sub-cultured  
97 in fresh LB broth for 4 h to late log phase (established by conventional counts of CFU). Prior to  
98 incubation with monocytes, bacteria were adjusted to a multiplicity of infection (MOI) of 10.

99 **Isolation of peripheral blood monocytes (PBM)**

100 Human blood was purchased from the blood transfusion service (Sheffield, UK). The blood was  
101 diluted with sterile PBS then gently poured onto Histopaque-1077, prior to isolation of the buffy  
102 coat, as standard procedure. After appropriate washing steps, buffy coat supernatants were  
103 resuspended with appropriate amounts of cold MACS buffer and anti-CD14 antibody coated  
104 micromagnetic beads (Miltenyi Biotech, Bisley, Surrey UK) according to the manufacturer's  
105 instructions. The viability of isolated monocytes was assessed using Trypan blue (10% v/v) and  
106 was found to be > 90 % prior to use.

107 ***Salmonella* invasion assays**

108 Monocytes were firstly washed with sterile PBS prior to culture with *S. Typhimurium* 4/74 at a  
109 multiplicity of infection (MOI) of 10:1 at 37 °C and 5% CO<sub>2</sub> for 60 min with or without  
110 VIP (10<sup>-7</sup> M). The cells were then washed and cultured with RPMI media containing 100 µg/ml  
111 gentamycin and incubated for a further 60 min. The monocytes were washed and the media was  
112 substituted with RPMI containing 25 µg/ml of gentamycin for a further 2, 6 or 24 h post-  
113 infection (pi) in total. The cells were then washed three times with PBS at room temperature and  
114 then lysed using 1 % Triton X (Fisher Scientific LTD, Loughborough, UK) for 15 minutes at 37  
115 °C. Intracellular bacterial counts were determined by serial dilution at different time points of 2,

116 6 and 24h pi. Viable bacterial cell counts were measured as colony forming units per ml  
117 (CFU/ml). All counts were performed in triplicate on 5 separate occasions.

### 118 **PCR analysis**

119 RNA was purified from treated or control monocytes by standard methods, using Rneasy plus  
120 kits (Qiagen, Hilden, Germany). RNA quantity and quality were measured using a NanoDrop  
121 8000 spectrophotometer (Thermo Scientific, Warrington, UK) and was converted into  
122 complimentary DNA (cDNA) using a SuperScript first strand DNA synthesis kit (Invitrogen,  
123 Carlsbad, CA, USA). For quantitative PCR analysis primers and probes were designed using a  
124 universal probe library (Roche Diagnostics, Mannheim, Germany). A PCR reaction volume (20  
125  $\mu$ l) consisting of 10  $\mu$ l Light Cycler 480 Probes Master (Roche, Germany), 1  $\mu$ l of each forward  
126 and reverse primer (Eurofins MWG, Operon, Germany) and 0.2  $\mu$ l, labelled with Fluorescein and  
127 dark quencher dye. The total volume was adjusted to 20  $\mu$ l using PCR water. In negative control  
128 wells, PCR water was added instead of cDNA. Standard curves of target and reference genes  
129 were performed at dilution ranges between 1:10- 10<sup>5</sup>. Thermal cycles consisted of denaturing at  
130 95 °C for 10 min and 40 cycles of sample amplification at 95 °C for 10 secs, 60 °C for 30 secs,  
131 72 °C for 1 min and cooling at 40 °C for 30 secs, performed using a Roche applied sciences light  
132 cycler 480 (Roche, Germany). All data was normalised to unstimulated monocytes, or expression  
133 in uninfected mouse tissues for *in vivo* studies, and quantification was determined by comparison  
134 to the reference gene using the Pfaffl method (18). All primers and probes used in PCR are  
135 shown in Table 1.

### 136 **Immunofluorescence studies**

137 Freshly isolated monocytes ( $5 \times 10^5$ ) were cultured on glass cover slips (VWR International Ltd,  
138 Leighton Buzzard, UK) placed in 24 well culture dishes, for 6h. The monocytes were then

139 infected with *S. Typhimurium* (6h pi) or cultured with VIP ( $10^{-7}$  M) in RPMI media for 6h, or  
140 cultured for 6 h in RPMI media without bacteria or VIP (uninfected control). After 6h the  
141 monocytes were washed 3 times in PBS and fixed in paraformaldehyde (4% v/v) for 10 min at  
142 room temperature prior to permeabilization in Triton-X (Fisher Scientific, Loughborough, UK)  
143 (0.2% v/v) for 10 min. After washing 3 times in PBS, the monocytes were incubated at room  
144 temperature for 30 min in blocking buffer; bovine serum albumin (BSA) solution (3% w/v in  
145 PBS). After washing 3 times in PBS the monocytes were incubated for 60 min with appropriate  
146 primary antibody (300  $\mu$ l), washed 3 times in PBS and incubated with secondary antibody (300  
147  $\mu$ l) in the dark for 45 min on an end-to-end shaker. After a final washing step, the coverslips  
148 were placed onto microscope slides prior to adding Vectashield hard set mounting medium. All  
149 slides were examined using a TCS SP2 confocal microscope (Leica Microsystems, Heidelberg,  
150 Germany). Each panel shown in figures 3 and 4 are merged plane image captures 4  $\mu$ m below the  
151 cell surface. To prevent spectral overlap, Alexa 488 and Alexa 647 fluorophore conjugates were  
152 chosen and bypass filtering was applied to prevent bleed through. Laser intensity and detector  
153 gain were optimised and standardised throughout. Each experiment was repeated in triplicate on  
154 5 separate occasions. All primary and secondary antibodies used during the confocal analysis,  
155 together with suppliers are shown in Table 2.

## 156 **Flow cytometry**

157 *S. Typhimurium* infected monocytes (6h pi), monocytes cultured with VIP and monocytes  
158 cultured only in RPMI media (unstimulated controls) for 6h were centrifuged at 300 x g for 10  
159 min. The supernatant was discarded and the cell pellet was washed 3 times by resuspension in  
160 PBS and centrifugation at 300 x g for 10 min, repeated a further 2 times. Monocytes were either  
161 left non-permeabilised or permeabilised for 10 min in Triton-X (Fisher Scientific, UK) (0.2%

162 v/v) and washed a further 3 times prior to incubation at room temperature for 30 min in blocking  
163 buffer (PBS and BSA 3% w/v). After washing 3 times in PBS the monocytes were incubated for  
164 60 min with mouse anti-human VPAC1 IgG2a (300 µl), washed 3 times in PBS and incubated  
165 with rat anti-mouse IgG2a-Alexa-488 (300 µl) (Table 2) in the dark for 45 min on an end-to-end  
166 shaker. The monocytes were then washed 3 times prior to analysing antibody fluorescence using  
167 a FACScan flow cytometer (Becton Dickinson, NJ, USA). Gating of the cell populations were  
168 performed, according to journal guidelines, using CD14 expression (92% of the population) and  
169 side scatter (SSC). In FACS plots, quadrants were set according to fluorescence expressed by  
170 monocytes incubated only with secondary antibody (control) (lower left quadrant) and  
171 fluorescence in test cell populations were compared to these. Data analysis was performed using  
172 FACSDiva software (Becton Dickinson, USA). Each experiment was performed in triplicate on  
173 5 separate occasions.

#### 174 **Calmodulin 1 (CAM1) agonist and antagonist studies**

175 To investigate the effect of CAM1 on VPAC1 expression, freshly isolated monocytes ( $5 \times 10^5$ )  
176 were incubated for 2h with either the CAM1 agonist; calcium-like peptide 1 (CALP1) (20 µM)  
177 (Tocris Bioscience, Abingdon, UK) or the CAM1 antagonist; W-7 (30 µM) (Sigma-Aldrich,  
178 Poole, UK). The concentrations of agonist and antagonist chosen in these experiments were  
179 determined via dose response and output curves (data not shown). PCR and flow cytometry  
180 were then performed to assess VPAC1 expression in *S. Typhimurium* infected and uninfected  
181 monocytes, as stated above at 6h pi. Mean data was obtained from experiments performed in  
182 triplicate on 5 separate occasions.



183 **Statistical Analysis**

184 Two-tailed unpaired student's *t* test or one-way ANOVA were performed to determine  
185 significant differences between different groups (control negative, *S. Typhimurium* infected,  
186 with or without VIP) using Graph Pad Prism software. Bonferroni's multiple comparisons test  
187 was applied to examine significant difference between the means of more than two groups,  
188 following ANOVA. Significance values were determined at the 95% confidence limit ( $P < 0.05$ ).

189

190

191 **Results**

192 ***S. Typhimurium* increases VPAC1 expression**

193 High constitutive expression of VPAC1 was detected by RTPCR but following *S. Typhimurium*  
194 infection, expression of VPAC1 increased further (Fig 1A). *S. Typhimurium* significantly  
195 increased VPAC1 mRNA expression by around 5 fold above expression in resting monocytes ( $P$   
196  $<0.05$ ) but VPAC1 expression was not differentially expressed when monocytes were cultured  
197 with VIP (Fig 1B). After 6 and 24h pi, significantly more *S. Typhimurium* were recovered from  
198 infected monocytes which had been co-cultured with VIP, compared to infected monocytes  
199 without VIP ( $P <0.05$ ) (Fig 1C).

200 Following FACS analyses, we also detected a 50% increase in the immunoreactivity of VPAC1  
201 protein in the cytosol of monocytes after 6h pi with *S. Typhimurium*, which was highly  
202 significant ( $P <0.01$ ) when compared to VPAC1 protein in the cytosol of monocytes incubated  
203 with VIP or uninfected monocytes (Fig 2A and C). FACS analysis also showed thatVPAC1  
204 protein was increased on the surface of monocytes infected with *S. Typhimurium* by around 30%  
205 and this increase was also significant ( $P <0.05$ ) when compared to VPAC1 protein in the cytosol  
206 of monocytes incubated with VIP or uninfected monocytes (Fig 2B and D).

207 **Retrograde recycling of VPAC1 occurs following *S. Typhimurium* infection of monocytes**

208 Confocal microscopy showed that VPAC1 expression was similar in monocytes incubated with  
209 VIP to that in unstimulated monocytes (Fig 3A), this was low and was partially co-localized with  
210 the early endosome antigen 1 (EEA1) within the early/sorting endosome (SE). However, VPAC1  
211 immunofluorescent intensity was greatly increased and was strongly co-localized with EEA1  
212 following *S. Typhimurium* infection (Fig 3A). Following internalization of VPAC1 in the SE of  
213 *S. typhimurium*-infected monocytes, VPAC1 was trafficked from the SE to recycling endosomes  
214 (REs) associated with the TGN (retrograde trafficking). This was indicated by strong co-  
215 localization of VPAC1 with Rab11a (Fig 3B) and concomitant co-localisation of Rab11a with  
216 the trans-Golgi network (TGN), using TGN protein 46 (TGN46) as a marker Fig 3C).

217 ***S. Typhimurium* induces anterograde recycling of VPAC1 via Rab3a/CAM1.**

218 Further trafficking of VPAC1 in monocyte exosomes, following *S. Typhimurium* Infection, was  
219 indicated by strong co-localisation of VPAC1 with the membrane docking protein Rab3a (Fig  
220 4A) which was concomitantly co-localised with CAM1 (Fig 4B). Subsequent qPCR analysis  
221 showed that *S. Typhimurium* infection induced a >5 fold ( $P < 0.05$ ) increase in both Rab3A and  
222 CAM1 above that measured in unstimulated monocytes or monocytes cultured with VIP (Fig  
223 4C). Addition of a CAM1 agonist (CALP1) to cell cultures significantly increased VPAC1  
224 mRNA expression in *S. Typhimurium*-infected monocytes ( $P < 0.05$ ), whereas addition of a  
225 CAM1 antagonist (W-7) significantly decreased VPAC1 mRNA expression ( $P < 0.05$ ) (Fig 4D).  
226 FACS analyses also indicated a causal association between CAM1 and VPAC1 protein  
227 expression. These showed that expression of VPAC1 protein on the surface of *S. Typhimurium*-  
228 infected monocytes was increased by CALP1 and decreased by W-7 (Fig 5G-I) compared to  
229 uninfected monocytes (Fig 5A-C) or monocytes cultured with VIP (Fig 5D-F) and in both cases

230 these changes were significant ( $P < 0.05$ ). P- values were calculated by ANOVA analysis of  
231 mean expression detected for each experimental group (Shown in Fig 5K). A diagrammatic  
232 model of intracellular cycling of VPAC1, induced by *S. Typhimurium* infection, is shown in Fig  
233 5L.

234

## 235 **Discussion**

236 We show that *S. Typhimurium* increased expression of VPAC1 in human monocytes and this  
237 was associated with increased intracellular survival of the bacteria, when infected monocytes  
238 were co-cultured with VIP. This is in accordance with a study by Storka et al., (2013) (12) who  
239 reported a >30% increase in VPAC1 expression in monocytes isolated from human volunteers  
240 24h after infusion of lipopolysaccharide (LPS) from *Escherichia coli* and this was correlated  
241 with an increased concentration of VIP in plasma. However, at least some of this effect is  
242 probably due to increased monocyte survival (13, 19) but the effect is not merely due to LPS,  
243 which we found to induce lower levels of VPAC1 by both qPCR and FACS analyses compared  
244 to *Salmonella* infection (data not shown).

245 Murine studies have indicated that the immunosuppressive effect of VIP occurs uniquely via  
246 VPAC1 (11) and that VIP/VPAC1 interaction regulates production of inflammatory mediators  
247 associated with mortality in sepsis (8), which may have evolved to protect the host. However,  
248 studies using viable *Salmonella*, rather than LPS have shown that VIP down-regulates  
249 inflammatory mediators and increases *Salmonella* survival in human monocytes (13, 19) and  
250 murine macrophages (20). We therefore hypothesised that *S. Typhimurium* actively utilises the  
251 VPAC1/VIP axis for its own survival advantage.

252 We now show that *S. Typhimurium* not only increased VPAC1 mRNA and protein expression  
253 but also induced VPAC1 recycling to the cell membrane. The initial step in this process was  
254 internalization of VPAC1 into EEA-1-containing SE. EEA-1 is required for tethering, docking  
255 and fusion of the SE to Soluble NSF Attachment Protein Receptor (SNARE), which  
256 subsequently leads to endosomal shipment (21). A previous study has shown that internalisation  
257 and localisation of VPAC1 in the SE occurred in VPAC1 transfected CHO cells, following  
258 culture with VIP (22). However, in this latter study, VPAC1 was not recycled back to the cell  
259 membrane and in accordance with this, we show that VIP did not increase VPAC1 expression on  
260 the cell membrane.

261 Internalised proteins may be trafficked via the SE to late endosomes and lysosomes (which  
262 may prevent further recycling) or to the trans-Golgi network (TGN) (retrograde transport) which  
263 may sort the proteins into recycling endosomes (REs) for subsequent transport back to the cell  
264 membrane (anterograde transport) (23-24). This requires interaction with Ras-associated  
265 binding (Rab) proteins, which are small GTPases involved in intracellular trafficking of protein  
266 cargo from the SE to downstream endosomes, including the RE, and the docking of transport  
267 vesicles with membrane targets (25). In our study, *S. Typhimurium*-induced retrograde  
268 transport of VPAC1 was indicated by strong co-localisation of VPAC1 with Rab11a, one of the  
269 best studied markers of REs (26) and TGN protein 46 (TGN46). The TGN is the critical region  
270 on the Golgi apparatus, which collects and sorts newly synthesised proteins and proteins relayed  
271 to it from REs (27-28). Some bacterial toxins, such as Shiga toxin, produced by *Shigella*  
272 *dysenteriae* (29), HIV envelope protein (30) and the immunosuppressive HIV nef protein (31-32)  
273 are trafficked from the cell surface via retrograde transport. However, our study is the first to  
274 show that *S. Typhimurium* (or any other pathogen) induces retrograde transporting of VPAC1.

275 The results we obtained also suggested that *S. Typhimurium* induced anterograde transport of  
276 VPAC1 via CAM1/Rab3a. The importance of Ca<sup>2+</sup> in regulated exocytosis has been known for  
277 a number of years (33) and a study by MacKenzie et al., (34) also reported a positive correlation  
278 between Ca<sup>2+</sup> concentration and VPAC1 density. Ca<sup>2+</sup> binding by CAM1 forms Ca<sup>2+</sup>/CAM1  
279 complexes that bind to Rab3a, which subsequently causes switching of Rab3a from a GDP-  
280 bound (inactive form) to a GTP-bound (active) form (35). It is possible that the increase in  
281 CAM1 and Rab3a mRNA we show may increase calcium binding and active Rab3a and thus  
282 VPAC1 binding and transport to the cell membrane. Active Rab3a is a constituent protein in  
283 secretory vesicles within PC-12 cells and, in newly formed secretory vesicles associated with the  
284 TGN in pancreatic acinar cells (36) and is involved in the docking and exocytosis of secretory  
285 vesicles (37). Very little has been reported regarding Rab3a in immune cells but a study by Abu-  
286 Amer et al., (1999) (38) has shown that Rab3a expression is increased in murine bone marrow  
287 derived macrophages stimulated with LPS, although this was not studied in the context of  
288 VPAC1. We also show that *S. Typhimurium* (which contains LPS) significantly increased Rab3a  
289 and CAM1 mRNA expression in monocytes. Moreover, our results show a causal link between  
290 CAM1 and VPAC1 expression on the monocyte membrane. However, the effect of CAM1  
291 agonist or antagonist was not absolute, thus suggesting that other factors (possibly Rab3a itself)  
292 also directly affect VPAC1 expression on the monocyte surface.

293 Only a fraction of newly synthesised VPAC1 become inserted into cell membranes, due to  
294 conformational misfolding (16) and although *S. Typhimurium* infection increased VPAC1  
295 mRNA expression, it is possible that *S. Typhimurium*-induced recycling of VPAC1 via  
296 retrograde/anterograde pathways overcomes low surface expression due to misfolding. This

297 would facilitate greater interaction with the increased concentration of VIP in serum, as shown  
298 by Storka et al., (2013) (12).

299 In conclusion, *S. Typhimurium* exploits the VPAC1/VIP axis to increase survival in human  
300 monocytes, this is achieved, at least in part, by retrograde and anterograde recycling of VPAC1  
301 via CAM1.

### 302 **Acknowledgments**

303 We would like to thank Mr Scott Hulme for technical support.

304 **Funding support:** The work was funded by a University of Duhok / Kurdistan Region of Iraq  
305 scholarship awarded to BA.

306

### 307 **Conflict of interest**

308 The authors have none to declare.

309

### 310 **References**

- 311 1. Annane D, Bellissant E, Cavaillon JM. Septic shock. *Lancet* 2005; **365**:63-78.
- 312 2. Davis BH. 2005. Improved diagnostic approaches to infection/sepsis detection. *Expert Rev*  
313 *Mol Diagn* 2005; **5**:193-207.
- 314 3. Ward NS, Casserly B, Ayala A. The compensatory anti-inflammatory response syndrome  
315 (CARS) in critically ill patients. *Clin Chest Med* 2008; **29**:617-625.
- 316 4. Danikas DD, Karakantza M, Theodorou GL, Sakellaropoulos GC, Gogos CA. Prognostic  
317 value of phagocytic activity of neutrophils and monocytes in sepsis. Correlation to CD64 and  
318 CD14 antigen expression. *Clin Exp Immunol* 2008; **154**:87-97.
- 319 5. Cohen J. Sepsis and septic shock: inching forwards. *Clin Med* 2009; **9**:256-257.

- 320 6. Antonucci E, Fiaccadori E, Taccone FS, Vincent JL. Glucocorticoid administration in sepsis  
321 and septic shock: time for a paradigm change? *Minerva Anesthesiol* 2014; **80**:1058-1062.
- 322 7. Du BH, Eng J, Hulmes JD, Chang M, Pan YC, Yalow RS. Guinea pig has a unique  
323 mammalian VIP. *Biochem Biophys Res Commun* 1985; **128**:1093-1098.
- 324 8. Delgado M, Martinez C, Pozo D, Calvo JR, Leceta J, Ganea D, Gomariz RP. Vasoactive  
325 intestinal peptide (VIP) and pituitary adenylate cyclase-activation polypeptide (PACAP) protect  
326 mice from lethal endotoxemia through the inhibition of TNF- $\alpha$  and IL-6. *J. Immunol* 1999;  
327 **162**:1200-1205.
- 328 9. Lara-Marquez M, O'Doriso M, O'Doriso T, Shah M, Karacay B. Selective gene expression  
329 and activation-dependent regulation of vasoactive intestinal peptide receptor type 1 and type 2 in  
330 human T cells. *J. Immunol* 2001; **166**:2522-2530.
- 331 10. EL Zein, N, Corazza F, Sariban E. The neuropeptide pituitary adenylate cyclase activating  
332 protein is a physiological activator of human monocytes. *Cell Signal* 2006; **182**:162-173.
- 333 11. Delgado M, Marie JC, Martinez C, Abad C, Leceta J. Anti-inflammatory properties of the  
334 type 1 and type 2 vasoactive intestinal peptide receptors: role in lethal endotoxic shock. *Eur J.*  
335 *Immunol* 2000; **30**:3236-3246.
- 336 12. Storka A, Burian B, Führlinger G, Clive T, Crevenna R, Gsur A, Mosgöller W, Wolzt M.  
337 VPAC1 receptor expression in peripheral blood mononuclear cells in a human endotoxemia  
338 model. *J. Transl Med* 2013; **11**:117.
- 339 13. Askar B, Ibrahim H, Barrow PA, Foster N. Vasoactive intestinal peptide (VIP) differentially  
340 affects inflammatory immune responses in human monocytes infected with viable *Salmonella* or  
341 stimulated with LPS. *Peptides* 2015; **71**:188-195.

- 342 14. Boissard C, Marie JC, Hejblum G, Gespach C, Rosselin G. Vasoactive intestinal peptide  
343 receptor regulation and reversible desensitization in human colonic carcinoma cells in culture.  
344 *Cancer Res* 1986; **46**:4406–4413.
- 345 15. Nachtergaeel I, Gaspard N, Langlet C, Robberecht P, Langer I. Asn229 in the third helix of  
346 VPAC1 receptor is essential for receptor activation but not for receptor phosphorylation and  
347 internalization: comparison with Asn216 in VPAC2 receptor. *Cell Signal* 2006; **12**:2121-2130.
- 348 16. Langer I, Leroy K, Gaspard N, Brion JP, Robberecht P. Cell surface targeting of VPAC1  
349 receptors: evidence for implication of a quality control system and the proteasome. *Biochim*  
350 *Biophys Act* 2008; **1783**:1663-16672.
- 351 17. Rankin JD, Taylor RJ. The estimation of doses of *Salmonella typhimurium* suitable for the  
352 experimental production of diseases in calves. *Vet Rec* 1966; **78**: 706-707.
- 353 18. Pfaffl MW. A new mathematical model for relative quantification in real time RT-PCR.  
354 *Nucleic acids Res* 2001; **29**:e45.
- 355 19. Ibrahim H, Askar B, Barrow PA, Foster N. Dysregulation of JAK/STAT genes by vasoactive  
356 intestinal peptide (VIP) in Salmonella-infected monocytes may inhibit its therapeutic potential in  
357 human sepsis. *Cytokine* 2018; **105**:49-56.
- 358 20. Foster N, Hulme SD, Barrow PA. Vasoactive intestinal peptide (VIP) prevents killing of  
359 virulent and *phoP* mutant *Salmonella typhimurium* by inhibiting IFN-gamma stimulated NADPH  
360 oxidative pathways in murine macrophages. *Cytokine* 2006; **36**:134-140.
- 361 21. Christoforidis S, McBride HM, Burgoyne RD, Zerial M. The Rab5 effector EEA1 is a core  
362 component of endosome docking. *Nature* 1999; **397**: 621-625.



- 363 22. Langer I, Gaspard N, Robberecht P. Pharmacological properties of Chinese hamster ovary  
364 cells coexpressing two vasoactive intestinal peptide receptors (hVPAC1 and hVPAC2). *Br J*  
365 *Pharmacol* 2006; **148**:1051-1059.
- 366 23. Bonafacino JS, Rojas R. Retrograde transport from endosomes to the trans-Golgi network.  
367 *Nat Rev Mol Cell Biol* 2006; **7**:568-579.
- 368 24. Hsu VW, Prekeris R. Transport at the recycling endosome. 2010. *Curr Opin Cell Biol* 2010;  
369 **22**:528-534.
- 370 25. Bhui T, Roy JK. Rab 11 in disease progression. *Int J Mol Cell Med* 2015; **4**:1-8.
- 371 26. Van Ijzendoorn SC. Recycling endosomes. *J. Cell Sci* 2006; **119**:1679-1681.
- 372 27. Gu F, Crump CM, Thomas G. Trans-Golgi network sorting. *Cell Mol Life Sci* 2001; **58**:1067-  
373 1084.
- 374 28. Guo Y, Sirkis DW, Schekman R. Protein sorting at the trans-Golgi network. *Annu Rev Cell*  
375 *Dev Biol* 2014; **30**:169-206.
- 376 29. Lamaze C, Johannes L. Intracellular trafficking of bacterial and plant toxins. Comprehensive  
377 sourcebook of bacterial toxins. J.E. Alouf, M.R. Popoff (Eds.) (Third Edition), Academic Press,  
378 London (2006).
- 379 30. Lopez-Verges S, Camus G, Blot G, Beauvoir R, Benarous R, Berlioz-Torrent C. Tail-  
380 interacting protein TIP47 is a connector between Gag and Env and is required for Env  
381 incorporation into HIV-1 virions. *Proc. Natl. Acad. Sci. USA* 2006; **103**:14947-14952.
- 382 31. Blagoveshchenskaya AD, Thomas L, Feliciangeli SF, Hung CH, Thomas G. HIV-1 Nef  
383 downregulates MHC-I by a PACS-1 and PI3K-regulated ARF6 endocytic pathway. *Cell* 2002;  
384 **111**:853-866.

- 385 32. Chaudhry A, Das SR, Jameel J, George A, Bal V, Mayor S, Rath S. HIV-1 Nef induces a  
386 Rab11-dependent routing of endocytosed immune costimulatory proteins CD80 and CD86 to the  
387 Golgi. *Traffic* 2008; **9**:1925-1935.
- 388 33. Burgoyne RD, Morgan A. Ca<sup>2+</sup> and secretory vesicle dynamics. *Trends Neurosci* 1995;  
389 **18**:191–196.
- 390 34. MacKenzie CJ, Lutz E, McCulloch DA, Mitchell R, Harmar AJ. Phospholipase C Activation  
391 by VIP1 and VIP2 Receptors Expressed in COS 7 Cells Involves a Pertussis Toxin-Sensitive  
392 Mechanism. *Ann NY Acad Sci USA* 1996; **805**: 579-584.
- 393 35. Park J-B, Kim J-S, Kim J-Y, Lee J-Y, Jaebong J-B, Kim J-Y, Seo J-Y, Kim A-R. GTP binds  
394 to Rab3A in a complex with Ca<sup>2+</sup>/calmodulin. *Biochem. J* 2001; **362**:651–657.
- 395 36. Jena BP, Gumkowski FD, Konieczko EM, von Mollard GF, Jahn R, Jamieson JD.  
396 Redistribution of a rab3-like GTP-binding protein from secretory granules to the Golgi complex  
397 in pancreatic acinar cells during regulated exocytosis. *J Cell Biol* 1994; **124**: 43-53.
- 398 37. Schlüter OM, Khvotchev M, Jahn R, Südhof TC. Localization versus function of Rab3  
399 proteins. Evidence for a common regulatory role in controlling fusion. *J. Biochem* 2002;  
400 **277**:40919-4029.
- 401 38. Abu-Amer Y, Teitelbaum SL, Chappel JC, Schlesinger P, Ross FP. Expression and  
402 regulation of RAB3 proteins in osteoclasts and their precursors. *J Bone Miner Res* 1999;  
403 **14**:1855-1860.

404

405

406

407

408

409

410

411

412

413 **Figure Legends**

414

415 **Table 1. Forward and reverse primers and probes used in PCR reactions.**

416 Forward and reverse primers and probes are shown for each gene analysed by PCR.

417

418 **Table 2. Primary and secondary antibodies used in confocal microscope analysis and flow**  
419 **cytometry.**

420 The type and concentration of primary and secondary antibodies, together with secondary  
421 antibody fluorophore conjugates, together with commercial suppliers, are shown.

422

423

424 **Figure 1. Increased survival of *S. Typhimurium* 4/74 in human monocytes co-cultured with**  
425 **VIP is associated with increased expression of VPAC1.**

426 Reverse transcription (rt) PCR showing constitutive and *S. Typhimurium*-induced expression of  
427 VPAC1 in monocytes after 6h post-infection (pi.). Comparison between VPAC1 expression is  
428 also shown with the reference gene  $\beta$ -actin, which is unchanged in both uninfected and infected  
429 monocytes. (B) Quantitative PCR (qPCR) showing expression of VPAC1 after 6h pi in  
430 monocytes infected with *S. Typhimurium* or cultured with VIP ( $10^{-7}$  M). Fold changes are

431 expressed in comparison with mRNA expression measured in unstimulated (control) monocytes,  
432 assigned an arbitrary expression value of 1. (C) Recovery of *S. Typhimurium* from monocytes  
433 cultured with or without VIP ( $10^{-7}$  M) at different times post-infection (pi). White bar = 2h pi,  
434 Grey bar = 6h pi, Black bar = 24h pi. Histograms (B and C) show means calculated from 5  
435 separate experiments performed in triplicate. Connecting bars show significant differences at  $P =$   
436 0.05, error bars show standard deviation from the mean.

437

438 **Figure 2. *S. Typhimurium* 4/74 increases VPAC1 protein in the cytosol and cell membrane**  
439 **of human monocytes.**

440 VPAC1 expression is shown in representative FACS analyses of 5 independent experiments  
441 performed in (A) the cytoplasm (permeabilised) and (B) cell membrane (non-permeabilised) at 6h  
442 pi. In all cases, lower left quadrants were set according to fluorescence expressed by monocytes  
443 incubated with secondary antibody only (control). Histograms show mean population sizes  
444 expressing VPAC1 after each treatment; permeabilised monocytes (C) and non-permeabilised  
445 monocytes (D) calculated from 5 independent experiments performed in triplicate. Connecting  
446 bars show significant differences at  $P = 0.01-0.05$ , error bars show standard deviation from the  
447 mean.

448

449 **Figure 3. *S. Typhimurium* infection stimulates retrograde transported of VPAC1 from**  
450 **early/sorting endosome to Rab11a-containing recycling endosome localized with the trans-**  
451 **Golgi network in human monocytes.**

452 Confocal Laser Scanning Microscopy showing co-localization of VPAC1 with EEA1 and  
453 Rab11a in human monocytes, each panel shows a merged plane image 4  $\mu\text{m}$  below the cell

454 surface. (A) Co-localization of VPAC1 immunofluorescence (green Alexa 488) with early  
455 endosome antigen 1 (red Alexa 647) (white arrows) with increased levels of VPAC1/EEA1  
456 association in *S. Typhimurium* infected monocytes at 6h pi.

457 (B) Co-localisation of VPAC1 (green Alexa 488) with Rab11a (red Alexa 647) (white arrows) is  
458 shown only in *S. Typhimurium* infected cells and in (C) co-localisation of Rab11a (red Alexa  
459 647) with TGN46 (green Alexa 488) (white arrows) is shown only in *S. Typhimurium* infected  
460 cells. CLSM images shown are representative of 5 independent experiments performed in  
461 triplicate. Scale bar (bottom left) = 20  $\mu$ m.

462

463 **Figure 4. *S. Typhimurium* 4/74 induces packaging of VPAC1 within Rab3a/CAM1**  
464 **containing secretory vesicles for anterograde transport to the cell membrane of human**  
465 **monocytes.**

466 (A-B) Confocal Laser Scanning Microscopy showing co-localization of VPAC1 with Rab3a and  
467 CAM1. Each panel shows a merged plane image 4  $\mu$ m below the cell surface.

468 (A) Co-localisation of VPAC1 (green Alexa 488) with Rab3a (red Alexa 647) (white arrows) in  
469 *S. Typhimurium* infected monocytes. (B) Co-localisation of CAM1 (green Alexa 488) with  
470 Rab3a (red Alexa 647) (white arrows) in *S. Typhimurium* infected monocytes. Images shown are  
471 representative of 5 independent experiments performed in triplicate. Scale bar (bottom left) = 20  
472  $\mu$ m. (C) qPCR showing increased expression of Rab3a and CAM1 mRNA in monocytes 6h pi  
473 with *S. Typhimurium*. (D) qPCR showing fold changes in VPAC1 mRNA with or without CAM1  
474 agonist (CALP1) or antagonist (W-7). Each bar is a mean of 5 independent experiments  
475 performed in triplicate. White bar = Without agonist/antagonist, Black bar = + CALP1 (agonist),  
476 Grey bar = + W-1 (antagonist). Connecting bars show significant differences at  $P = 0.05$ , error

477 bars show standard deviation from the mean. Fold changes are expressed as a comparison with  
478 mRNA expression measured in unstimulated (control) monocytes after 6h, assigned an arbitrary  
479 expression value of 1.

480

481 **Figure 5. CAM1 increases VPAC1 protein expression on the cell membrane of monocytes**  
482 **infected with *S. Typhimurium* 4/74.**

483 (A-J) FACS analysis showing VPAC1 expression on the monocyte membrane 6h pi with *S.*  
484 *Typhimurium* or monocytes cultured with VIP ( $10^{-7}$  M) for 6h, with or without CAM1 agonist  
485 (CALP1; 20 $\mu$ g/ml) or CAM1 antagonist (W-7; 30  $\mu$ g/ml). FACS analyses shown are  
486 representative of experiments performed in triplicate on 5 separate occasions. Y-axes, SSC =  
487 Side scatter, X-axis = VPAC1 expression. Quantitative analysis of experimental means are  
488 shown in (K). Black bars = 2h post-treatment treatment/infection, White bars = 6h post-  
489 treatment/infection and Grey bars = 24h post-treatment/infection. Connecting bars show  
490 significant differences at P = 0.05, error bars show standard deviation from the mean.

491 (L) Diagrammatic representation of *S. Typhimurium* induced trafficking of VPAC1 receptors. (1)  
492 *S. Typhimurium* invades monocyte. (2) VPAC1 is packages in the EEA1 positive sorting  
493 endosome (SE). (3) Retrograde transport of VPAC1 occurs via Rab11a positive recycling  
494 endosome (RE) which is associated with TGN46 on the Golgi apparatus. (4) Anterograde  
495 transport of VPAC1 occurs via Rab3a/CAM1 positive secretory vesicle (SV).

496

497

498

499

500

501

502

Fig 1. Askar et al

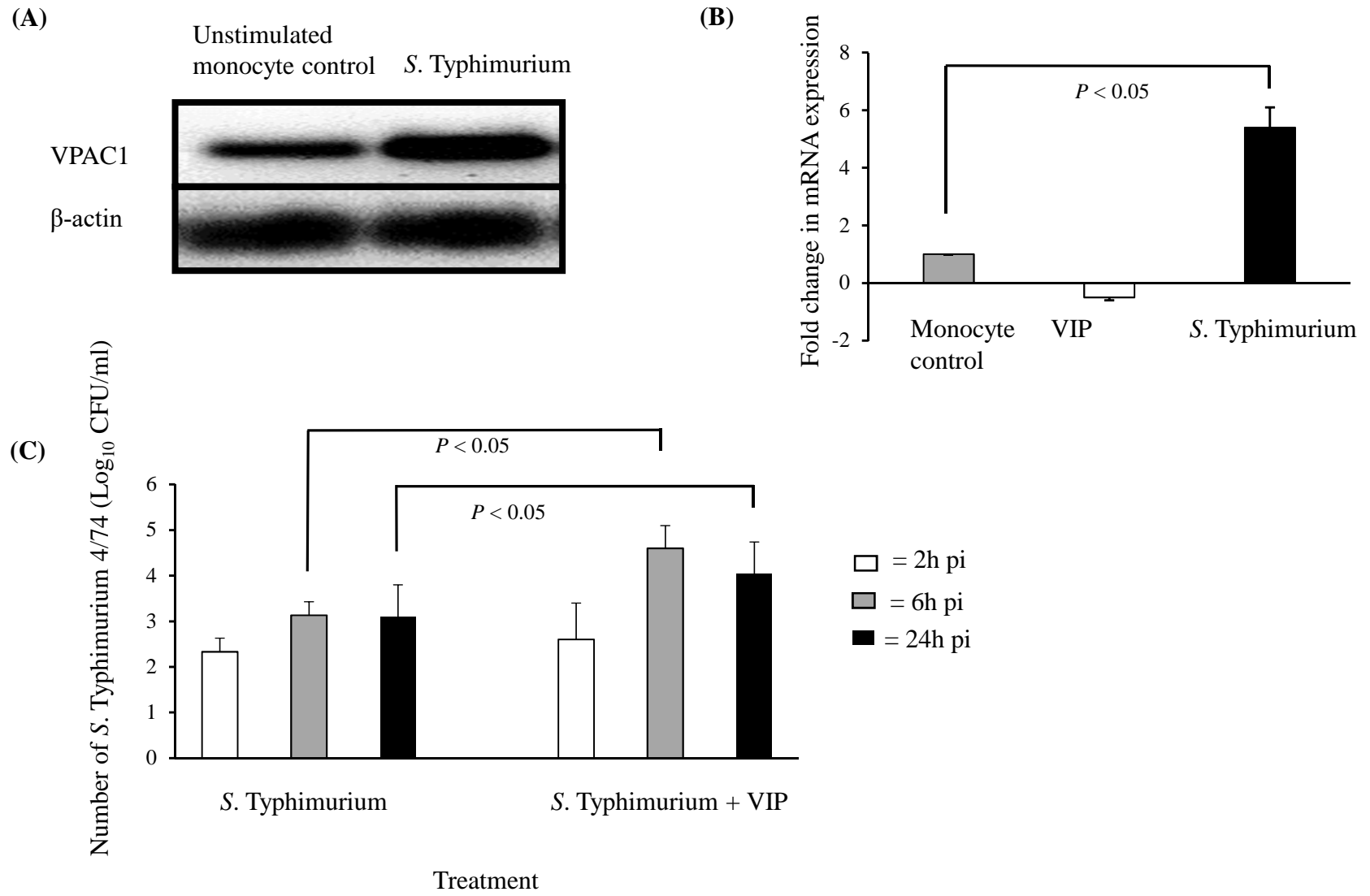




Fig 2. Askar et al

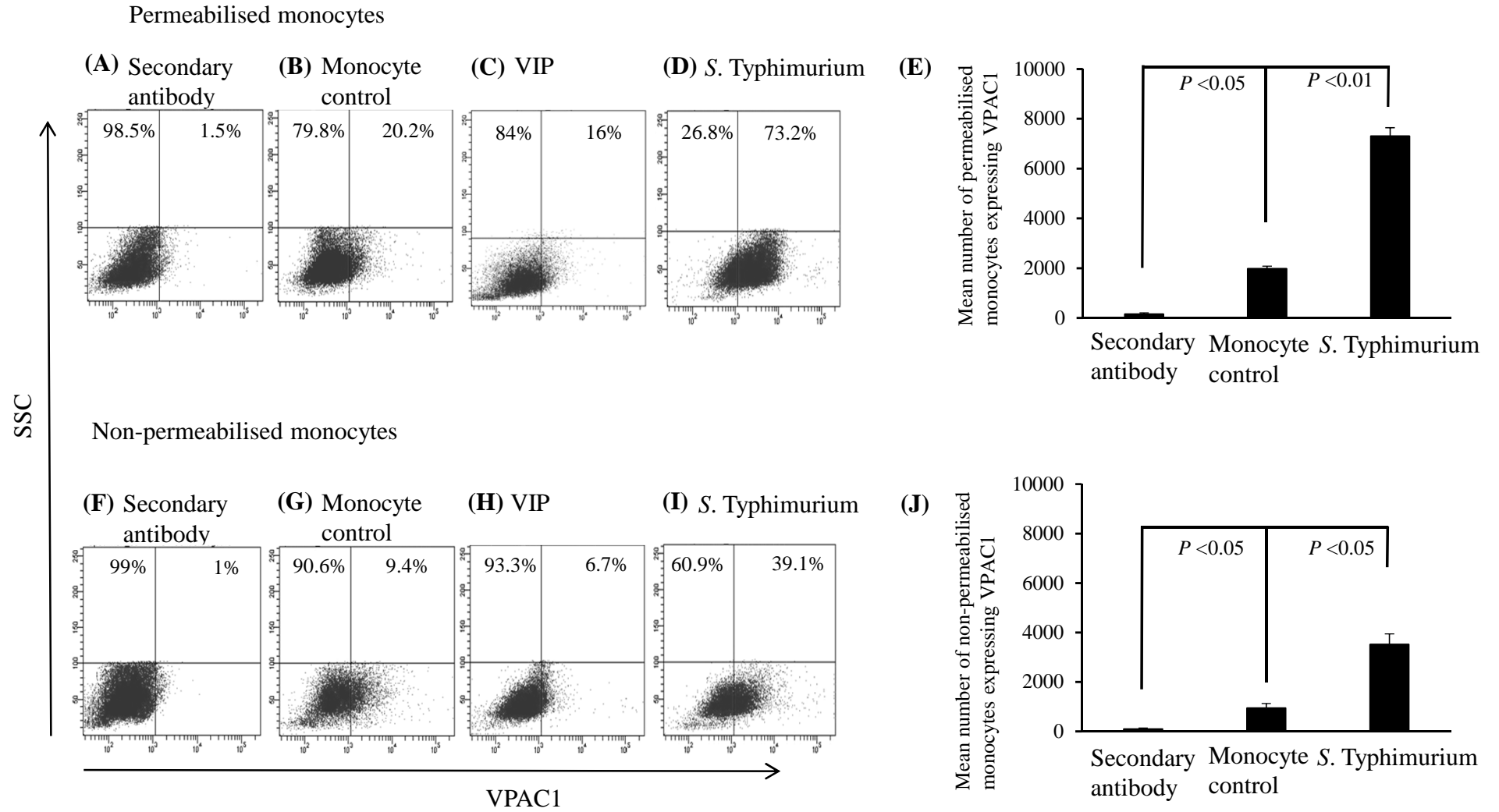


Fig 3. Askar et al

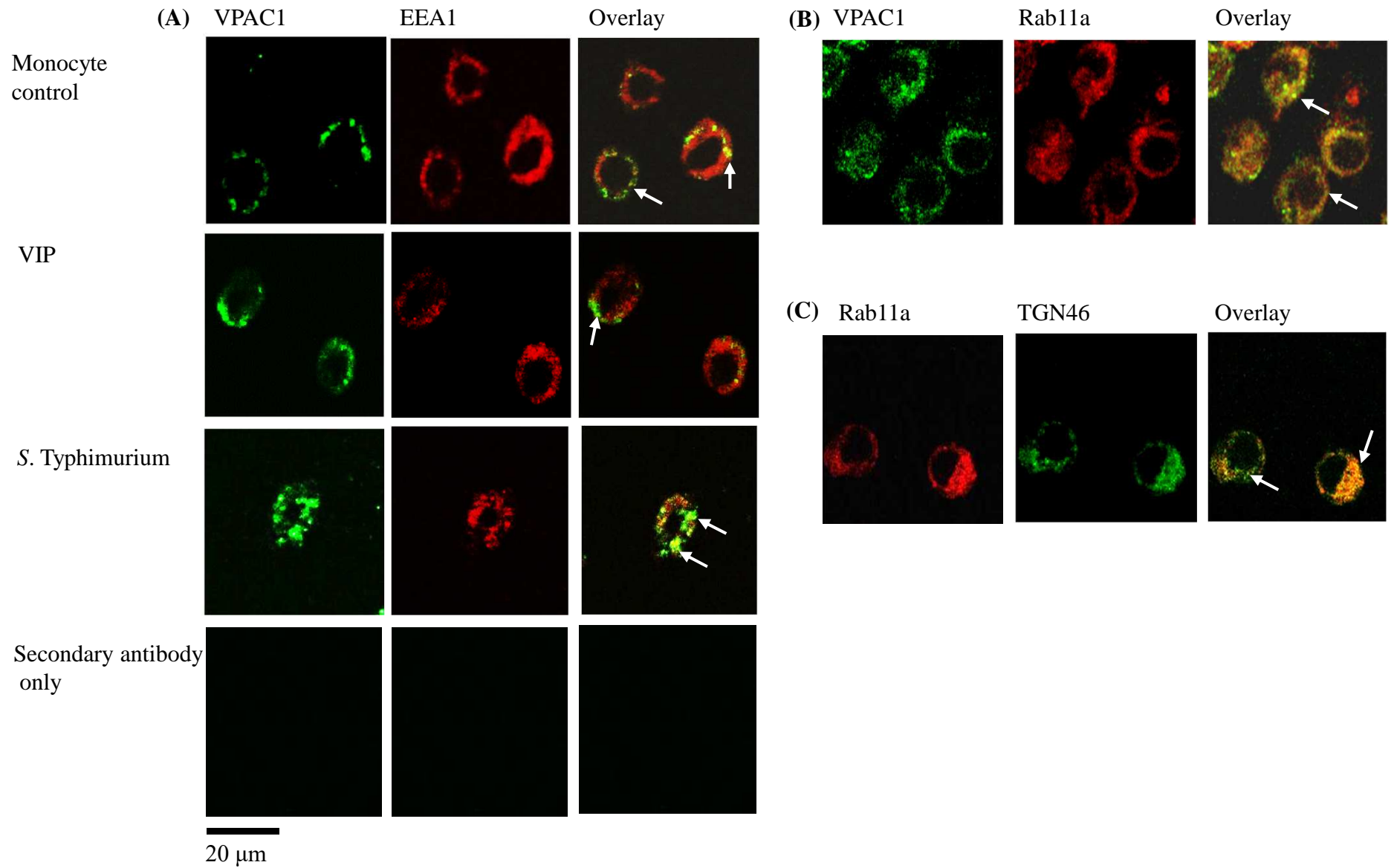
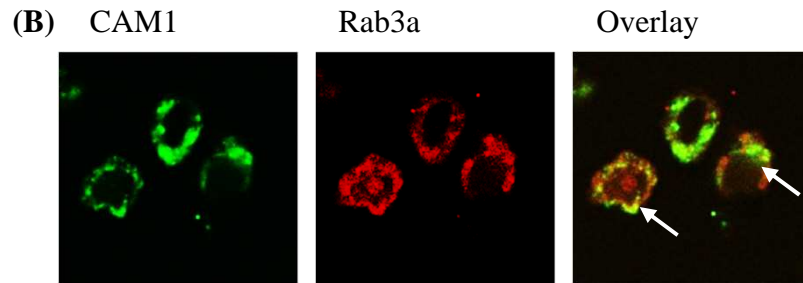
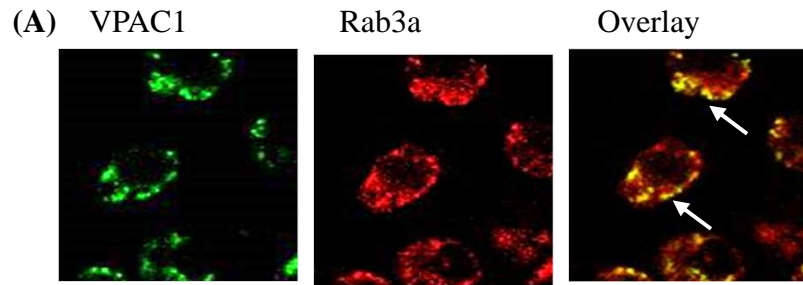


Fig 4. Askar et al



20  $\mu$ m

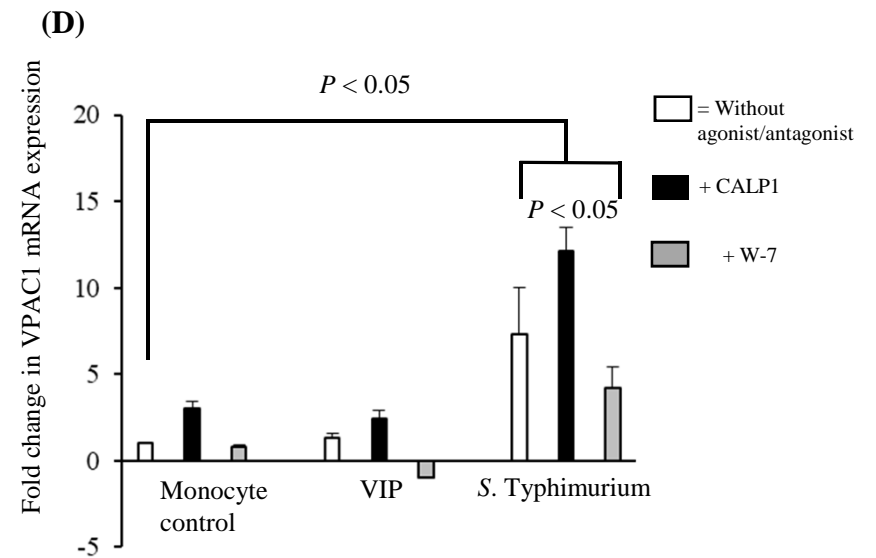
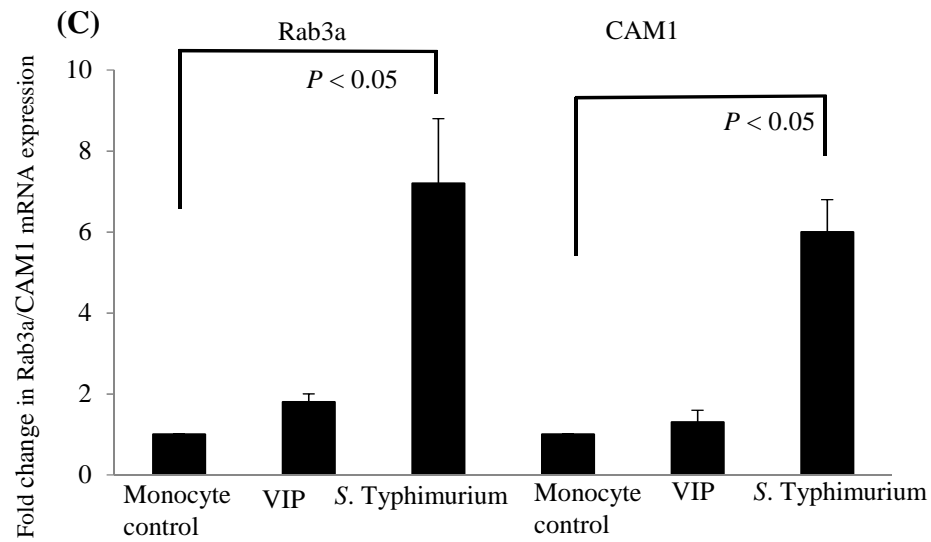


Fig 5. Askar et al

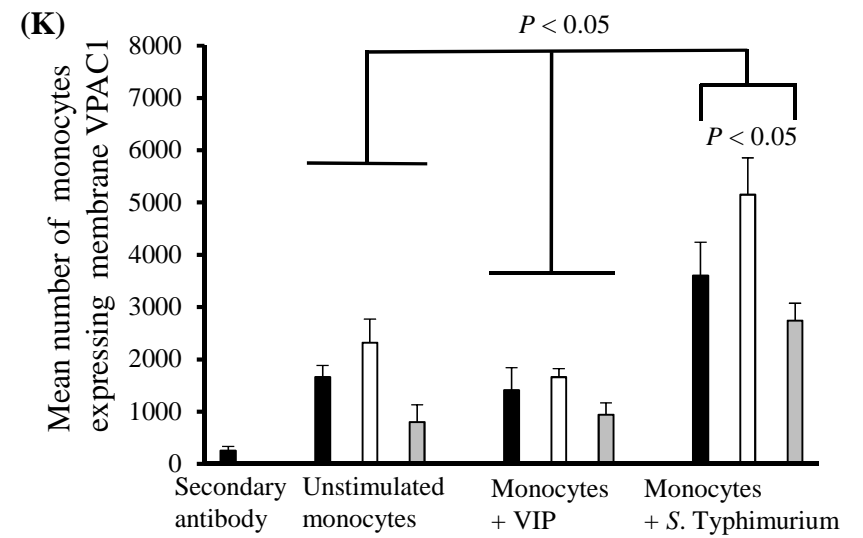
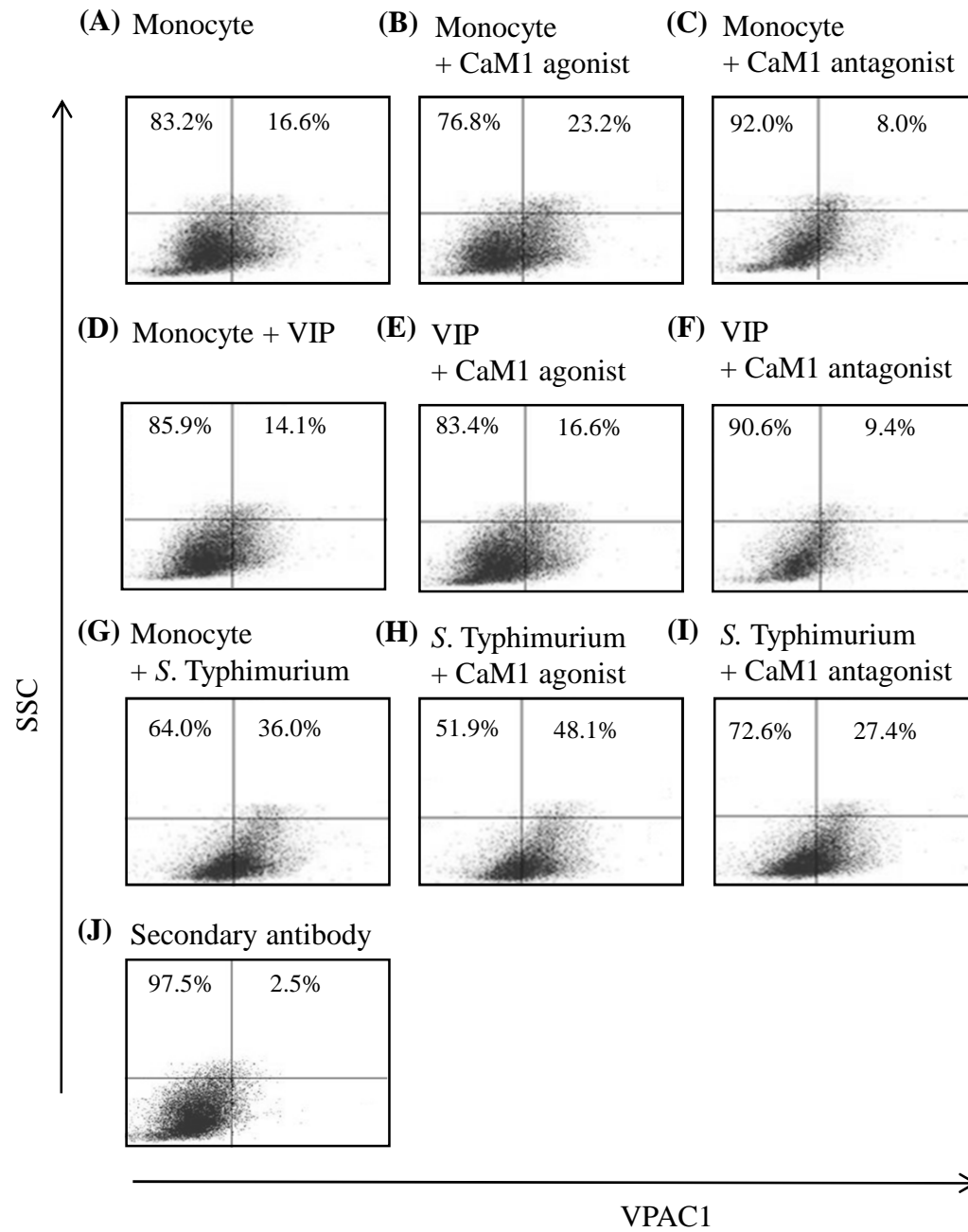


Fig 5. Askar et al

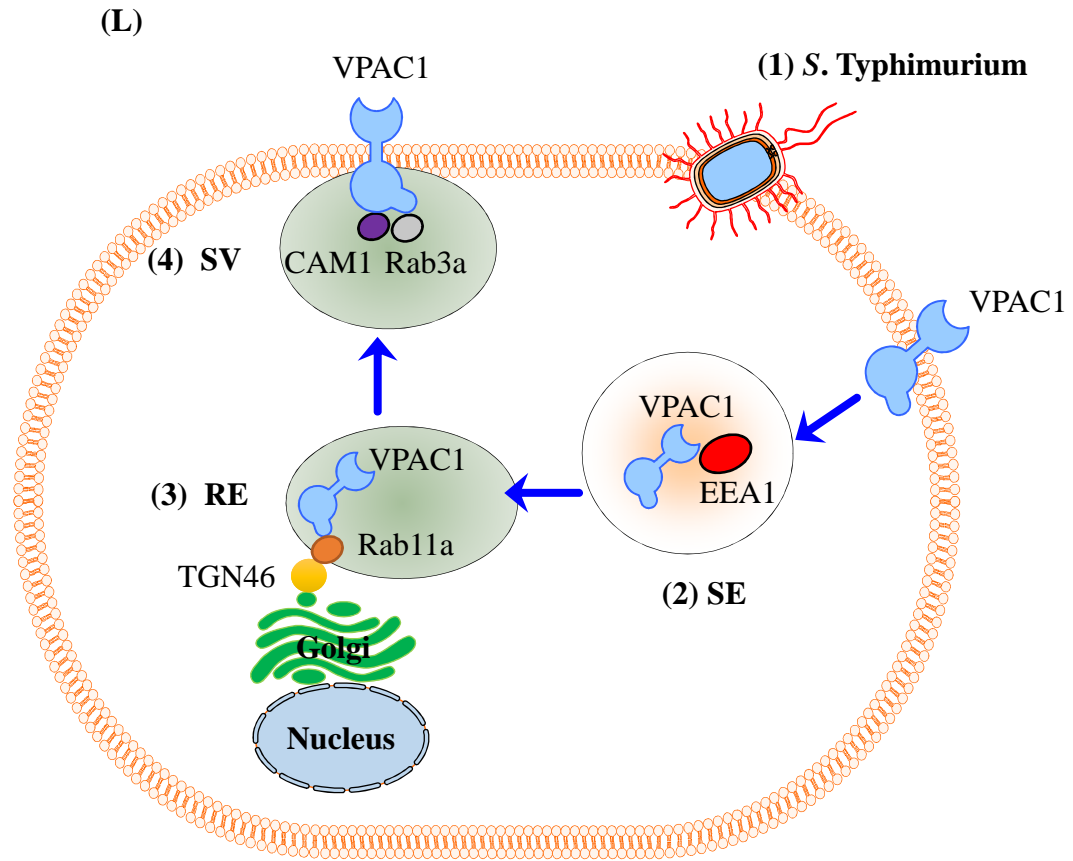


Table 1. Askar et al

<b>Gene</b>	<b>Forward primer (5'-3')</b>	<b>Reverse primer (3'-5')</b>	<b>Probe</b>
<b>VPAC1</b>	TCCGCCAGC CACTCTATC	GCTCGAGCC TGCACAATC	#19
<b>Rab3a</b>	AACGAGGAA TCCTTCAATGCA	TGGGCATTGT CCCATGAGTA	TGCAGGACTGGT CCACCCAGATCA
<b>CAM1</b>	TGCATTCAGGGC TGATTTATAGAG	AACAAGCTACAA AATGCCAGAAAGA	CCCTTGGCTTCTC CTTCTCCTACTCCCT
<b>β-actin</b>	CCAACCGCG AGAAGATGA	CCAGAGGAGT ACAGGGATAG	#64

Table 2. Askar et al

<b>Receptor</b>	<b>Primary antibody</b>	<b>Conc. (<math>\mu\text{g/ml}</math>)</b>	<b>Secondary antibody</b>	<b>Conc. (<math>\mu\text{g/ml}</math>)</b>
<b>VPAC1</b>	Mouse anti-human IgG2a (Abcam, Camb, UK)	1	Rat anti-mouse IgG2a-Alexa 488 (Abcam, Camb, UK)	0.1
<b>EEA1</b>	Rabbit anti-human IgG (Abcam, Camb, UK)	1	Donkey anti-rabbit IgG-Alexa 647 (Abcam, Camb, UK)	2
<b>Rab3a</b>	Rabbit anti-human IgG (Abcam, Camb, UK)	1	Donkey anti-rabbit IgG-Alexa 647 647 (Abcam, Camb, UK)	2
<b>CAM1</b>	Mouse anti-human IgG1 (Abcam, Camb, UK)	2	Rat anti-mouse IgG1-Alexa 488 (Invitrogen, Frederick, USA)	1
<b>Rab11a</b>	Rabbit anti-human IgG (Abcam, Camb, UK)	1	Donkey anti-rabbit IgG Alexa 647 647 (Abcam, Camb, UK)	2
<b>TGN46</b>	Mouse anti-human IgG1 (Abcam, Camb, UK)	5	Rat anti-mouse IgG1-Alexa 488 (Invitrogen, Frederick, USA)	1